

# Effect of Strong Ground Motion Duration on Structural Damage



**E.Özer & S.Soyöz**

*Department of Civil Engineering, Boğaziçi University, Turkey*

**M. Çelebi**

*U.S. Geological Survey, Menlo Park, CA, US*

## **SUMMARY:**

The goal of this study is to investigate the relationship between Strong Ground Motion Duration (SGMD) and structural damage. In literature, there exist numerous efforts regarding the effect of SGMD on structural damage. Several studies point out a positive correlation between SGMD and structural damage, while some others prove this wrong. In this study, a typical 5 storey building with a period of 0.5 seconds was idealized as a single-degree-of-freedom (SDOF) model. Its non-linear behavior was characterized by a bilinear hysteresis model. Initial stiffness value was calculated using the known period and representative mass of the structure; the secondary stiffness was assumed to be 20% of the initial stiffness. Yielding force was estimated by dividing the maximum elastic demand with a ductility factor of 4. Earthquake records with the magnitudes greater than 6 and the peak ground accelerations (PGA) greater than 0.2 g were used as input ground motions. In total, 179 earthquake records were selected from Peer Strong Motion Database and Strong Motion Center, and these records are grouped according to their PGA and frequency ranges. Arias Intensity was considered to define SGMD, and maximum non-linear displacement response was chosen as damage indicator. In general, there is a positive correlation between SGMD and damage; however, in some PGA and frequency ranges input motions with shorter durations may cause more damage than the input motions with longer durations.

*Keywords: Strong ground motion duration, non-linear SDOF*

## **1. INTRODUCTION**

There are three important characteristics of an earthquake motion; namely, amplitude, frequency content and duration. Amplitude represented with PGA has a direct impact but not necessarily the sole cause of structural damage. The same is true for frequency content; as the predominant frequency gets closer to natural frequency of the structure; damage probability increases but requires larger amplitude of input motion to be detrimental. On the other hand, SGMD and structural damage has no clear relation. In literature, there are numerous studies investigating the correlation between SGMD and structural damage. Paper by Hancock and Bommer (2006) reviews a large number of studies on the relation of these two parameters. They conclude that some researchers show a high correlation between SGMD and structural damage whereas some others find no relation. For example, a positive relation between number of cycles i.e. SGMD and structural damage is shown based on experimental testing (Dutta and Mander, 2001; Krawinkler, 1987; Park et.al, 1985). On the other hand, Iervolino (2006) finds no relation between SGMD and damage probability. Housner (1956) is the first researcher who states that energy input to the structure causes damage and is directly related with SGMD. Some other researchers also indicates positive relation between energy input and damage (e.g. Erberik and Sucuoglu, 2002; Uang and Bertero, 1990; Fajfar et.al, 1989). Researchers also suggest modifying elastic/inelastic response spectrum due to SGMD effects (Chai, 2005; Safak, 1998). In this study, maximum non-linear deformation of a SDOF system is obtained under 179 input ground motions including long-duration records from recent Japan and Chile earthquakes. SGMD and structural damage is correlated for different PGA and frequency ranges to exclude their effects. In the following sections, first, non-linear system characteristics and input motion selection are presented. Then, non-linear deformation and damage is correlated. Finally, some conclusions are made.

## 2. NON-LINEAR SDOF SYSTEM

In this study, a typical 5 storey building with a period of 0.5 seconds (0.1 seconds x number of storey) was idealized as a SDOF model. Its non-linear behavior was characterized by a bilinear hysteresis model. Initial stiffness value was calculated using the known period and representative mass of the structure; the secondary stiffness was assumed to be 20% of the initial stiffness. According to the design spectrum proposed by Turkish Earthquake Resistant Design Guideline (<http://www.csb.gov.tr/turkce/html/yonetmelik29.htm>) and system properties shown in Table 2.1, spectral acceleration corresponding to the period of 0.5 seconds is 1 g. As a result, maximum elastic demand could be evaluated as it is proportional with mass and spectral acceleration. Yielding force was estimated by dividing the maximum elastic demand by the ductility factor.

**Table 2.1.** System properties

Peak Ground Acceleration	0.4g
Importance Factor	1
Soil Type	Z3 ( $T_A=0.15$ s - $T_B=0.60$ s & $V_S\cong 300$ m/s)
Ductility	4 (Normal Ductility Level)

## 3. SELECTION OF INPUT MOTIONS

The content of the inputs is based on representing a wide range of real earthquakes which would cause considerable damage. Therefore, most of the available earthquake records with moment magnitude larger than 6, and peak horizontal acceleration larger than 0.2 g are considered. 179 records from Pacific Earthquake Engineering Research Center (<http://peer.berkeley.edu/smcat/search.html>) and Center for Engineering Strong Motion Data (<http://strongmotioncenter.org>) are used in the analyses as shown Table 3.1. In order to avoid dominance of an earthquake, number of records for each earthquake is limited.

**Table 3.1.** List of earthquakes

Earthquake Name	Location	Year	Mag.	Earthquake Name	Location	Year	Mag.
Cape Mendocino	CA, US	1992	7.2	Tabas	Iran	1978	7.7
Chalfant Valley	CA, US	1986	6.2	Taiwan	Taiwan	1986	6.4
Chi Chi	Taiwan	1999	7.7	Victoria	Mexico	1980	7.0
Coalinga	CA, US	1983	6.5	Whittier Narrows	CA, US	1987	6.0
Duzce	Turkey	1999	7.2	Big Bear	CA, US	1992	6.5
Erzincan	Turkey	1992	6.8	Sierra El Mayor	Mexico	2010	7.2
Friuli	Italy	1976	6.4	Chile	Chile	2010	8.8
Gazli	USSR	1976	6.8	Ferndale	CA, US	2010	6.5
El Centro	CA, US	1940	7.1	Hawaii	US	2006	6.7
Imperial Valley	CA, US	1979	6.4	Hector Mine	CA, US	1999	7.2
Irpinia	Italy	1980	6.8	Tohoku	Japan	2011	9.0
Kobe	Japan	1995	6.9	Japan-a	Japan	2011	7.1
Kocaeli	Turkey	1999	7.6	Japan-b	Japan	2011	6.6
Landers	CA, US	1992	7.3	Iwaki Offshore	Japan	2011	6.3
Loma Prieta	CA, US	1989	6.9	Shizuoka Offshore	Japan	2011	6.2
Mammoth Lakes	CA, US	1980	6.1	Long Beach	CA, US	1933	6.4
Morgan Hill	CA, US	1984	6.2	New Zealand	N. Z.	2010	7.0
Nahanni	Canada	1985	6.8	New Zealand	N. Z.	2011	6.3
Northridge	CA, US	1994	6.7	Park Field	CA, US	2004	6.0
Palm Springs	CA, US	1986	6.1	Petrolia	CA, US	1991	6.0
Park Field	CA, US	1966	6.1	Petrolia	CA, US	1992	7.1
San Fernando	CA, US	1971	6.7	Petrolia (aftershock)	CA, US	1992	6.5
Santa Barbara	CA, US	1978	6.0	Petrolia (aftershock)	CA, US	1992	6.6
Superstition Hills	CA, US	1987	6.7	Sumatra	Indonesia	2007	8.5

For the purpose of cancelling out all of strong motion parameters but duration, selected records are split into groups according to their predominant frequency and PGA values. As a result, each set of records consists of similar frequency and amplitude content, but differs in duration. Figure 3.1 and 3.2 show time history and frequency content of two different motions with similar PGA's but different frequency content. Frequency content of an input motion can be determined either by peak or predominant frequency as shown in Figure 3.3. It can be clearly seen that peak and predominant frequency criteria give different values. In this study, input motions with all frequency content were chosen; however, in the following sections, grouping of the input motions is based on peak frequency criteria. Table 3.2 shows the number of input motions for each group of PGA and frequency range.

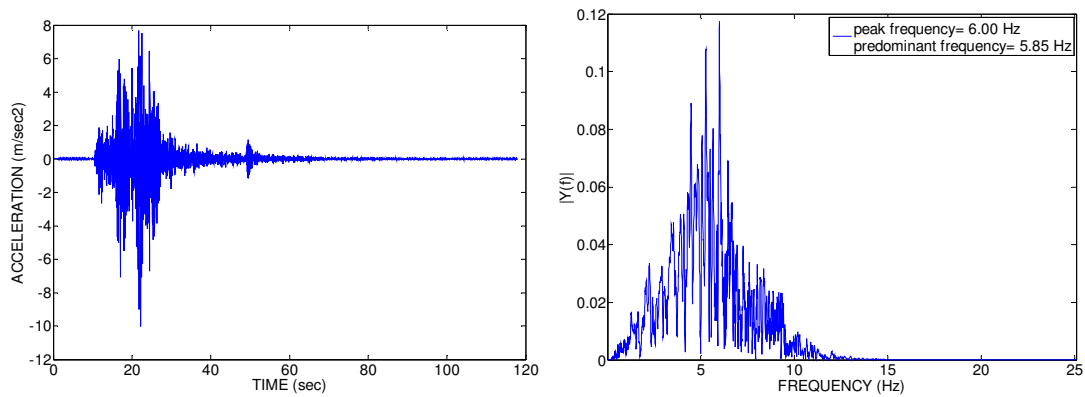


**Figure 3.1.** Time history and Fourier amplitude of Hawaii Earthquake (2006)

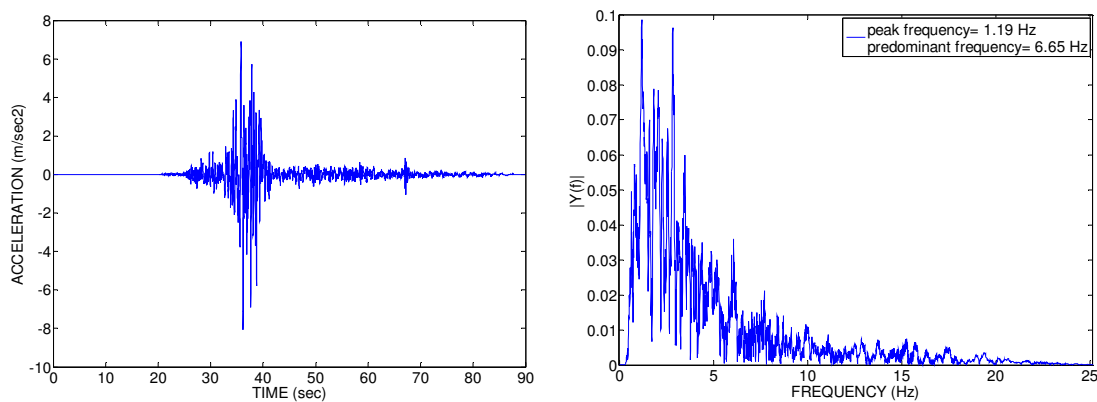


**Figure 3.2.** Time history and Fourier amplitude of Chi-Chi Earthquake (1999)

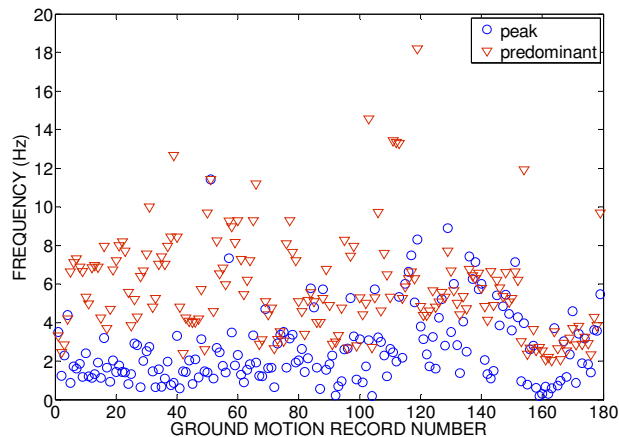


**Figure 3.3.** Peak and predominant frequencies of input motions

**Table 3.2.** Number of earthquakes for each PGA and frequency range

	PGA<4	4<PGA<6	6<PGA<8	8<PGA<10	10<PGA<12	12<PGA
0.0<F<0.4	3	1	0	1	0	0
0.4<F<0.8	6	4	2	1	0	0
0.8<F<1.2	10	6	3	1	1	0
1.2<F<1.6	8	7	3	4	2	2
1.6<F<2.0	8	8	1	2	1	1
2.0<F<2.4	5	5	2	1	0	1
2.4<F<2.8	4	5	2	0	0	1
2.8<F<3.2	6	3	1	2	0	3
3.2<F<3.6	4	0	4	2	1	3
3.6<F<4.0	0	3	0	1	0	1
4.0<F<4.4	2	0	0	1	0	1
4.4<F<4.8	1	0	2	0	0	1
4.8<F<5.2	0	2	0	0	0	0
5.2<F<5.6	4	1	1	0	0	0
5.6<F<6.0	2	0	0	2	1	0
6.0<F<6.4	0	0	1	0	0	2
6.4<F<6.8	0	0	1	0	0	0

#### 4. DURATION AND DAMAGE RELATION

In literature, there exist numerous definitions of SGMD; and consideration of different definition could lead different results. In this study, Arias intensity is used to determine SGMD. Arias intensity is based on energy released by the ground motion input. The strong motion portion of an input is defined as the 90 % of the total input. The beginning and ending time is defined as 5% and 95 %, respectively. Figure 4.1 shows the Arias intensity of Hawaii Earthquake (2006).

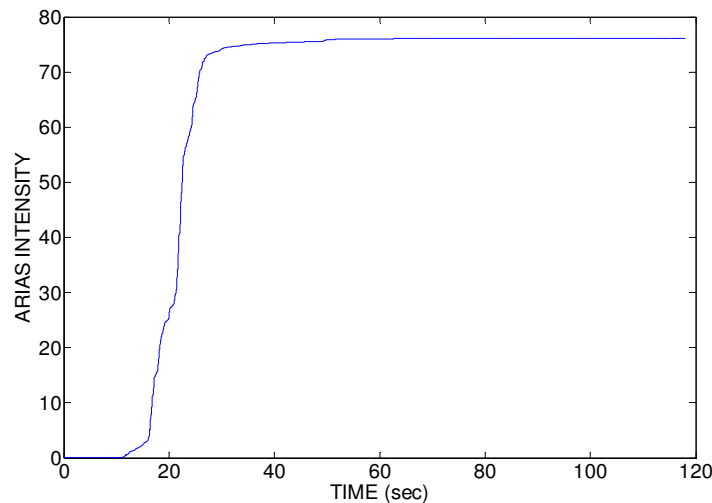


**Figure 4.1.** Arias intensity of Hawaii Earthquake

Non-linear time history analyses under given earthquake input motions were carried out in OpenSees platform. For damage assessment, maximum non-linear displacement was considered as the damage indicator of the structure. Figure 4.2 shows the non-linear response of the system under Hawaii Earthquake (2006).

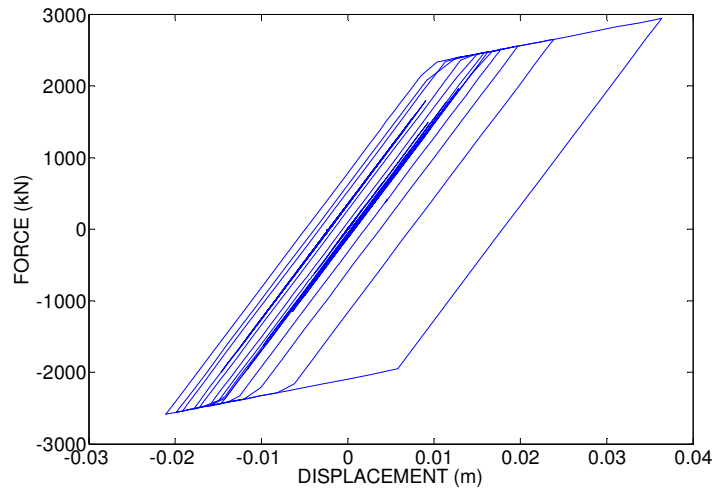


**Figure 4.2.** Force deformation relationship for Hawaii Earthquake

Figure 4.3 is the surface plot for Displacement-Duration-Frequency and Figure 4.4 is the surface plot for Displacement-Duration-PGA. Based on these two figures, there is no clear relation between maximum non-linear displacement (damage) and duration due to large non-linear displacements for short duration motions. For example, in Figure 8, larger non-linear displacements occur at short durations and low frequencies and in Figure 9 larger non-linear displacements are at short duration and moderate PGA levels. On the other hand, in both figures, there is another dimension not included i.e. PGA is not included Displacement-Duration-Frequency plot and Frequency is not included in Displacement-Duration-PGA plot. Therefore, results are reformatted through Figures 4.5-4.8 in which maximum non-linear displacement and duration is presented for each PGA and frequency range i.e. PGA and frequency content are no more a parameter. Based on these four figures, it can be concluded that maximum non-linear displacement has a positive relation with SGMD.

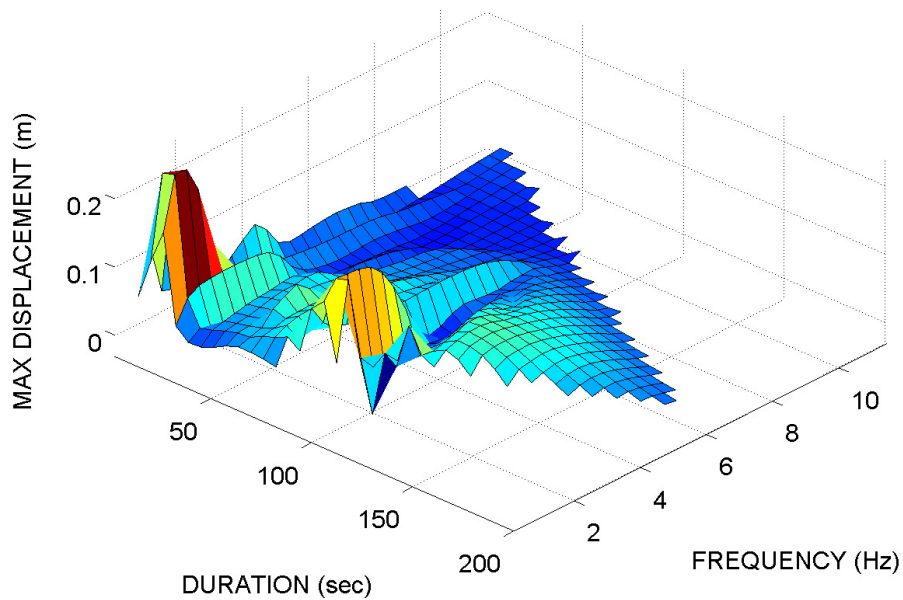


**Figure 4.3.** Displacement-Duration-Frequency relationship

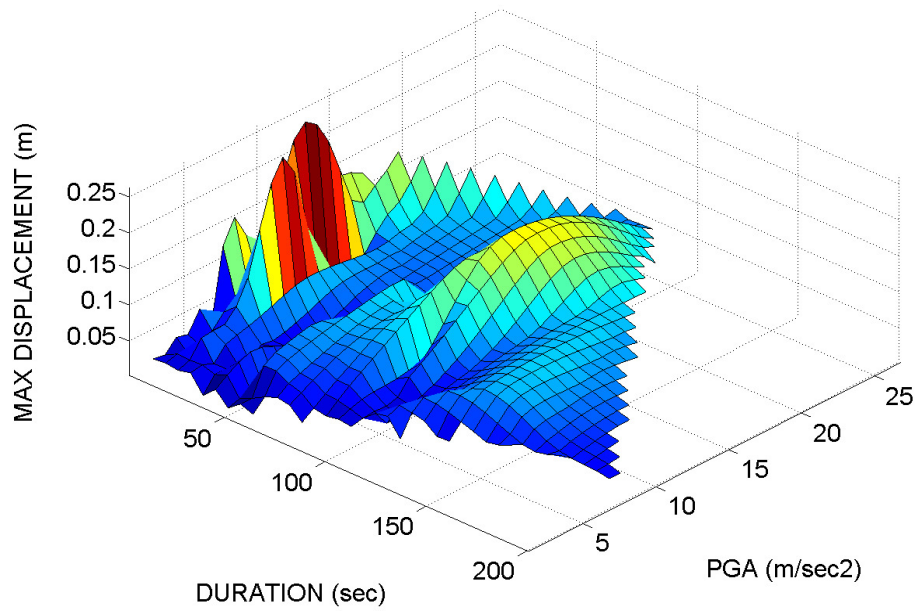


**Figure 4.4.** Displacement-Duration-PGA relationship

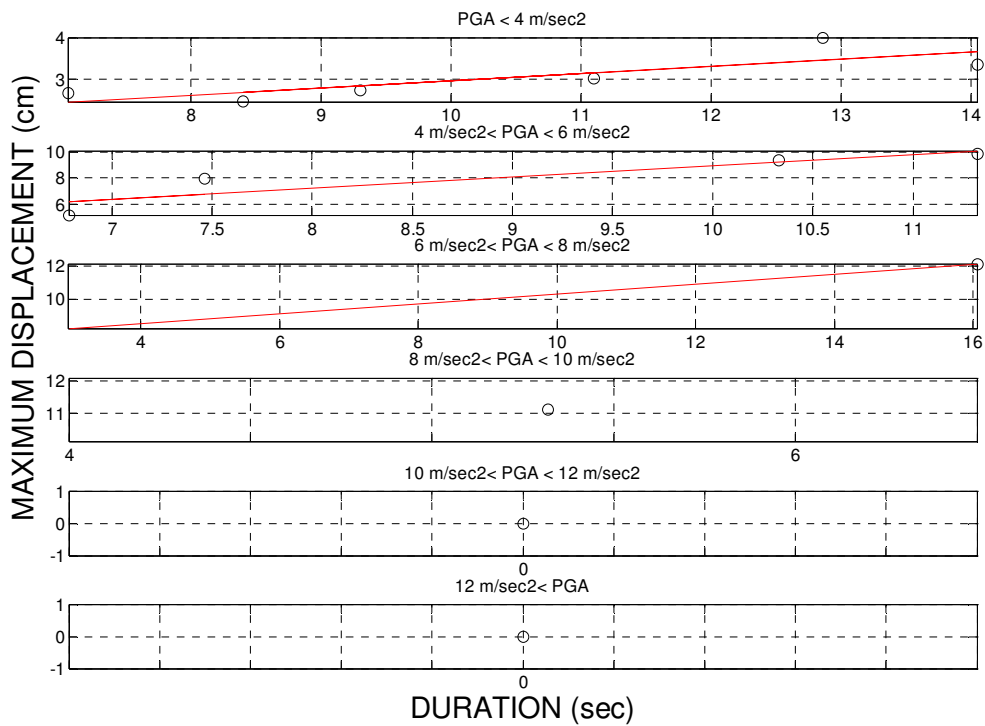


**Figure 4.5.** Max. Non-linear Displacement and SGMD relationship (frequency content of input motion is between 0.4-0.8 Hz)

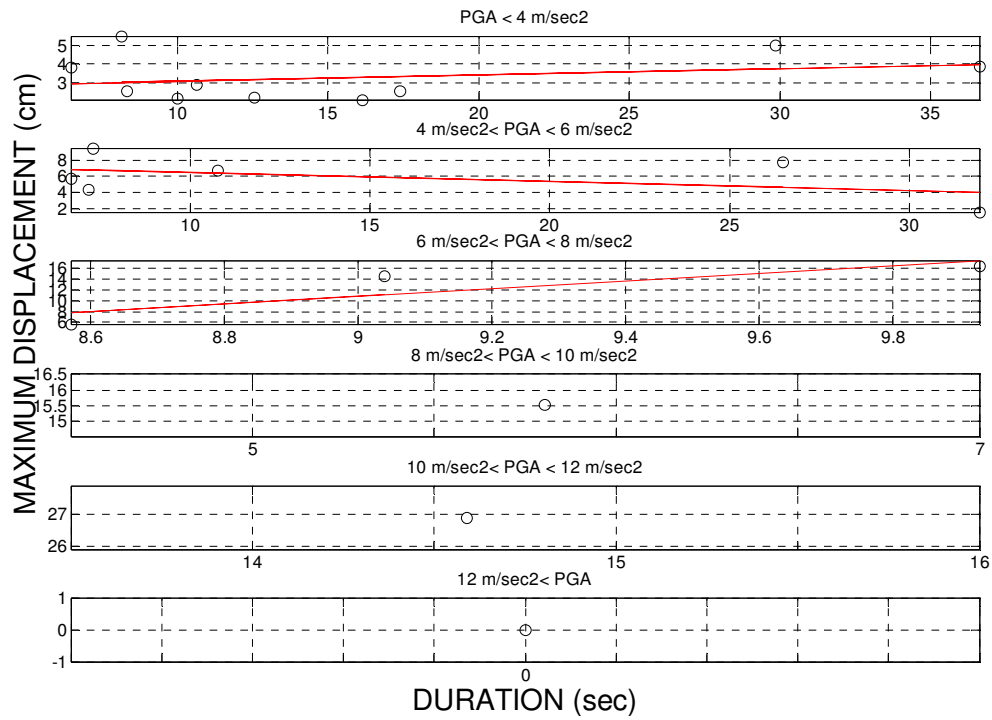


**Figure 4.6.** Max. Non-linear Displacement and SGMD relationship (frequency content of input motion is between 0.8-1.2 Hz)

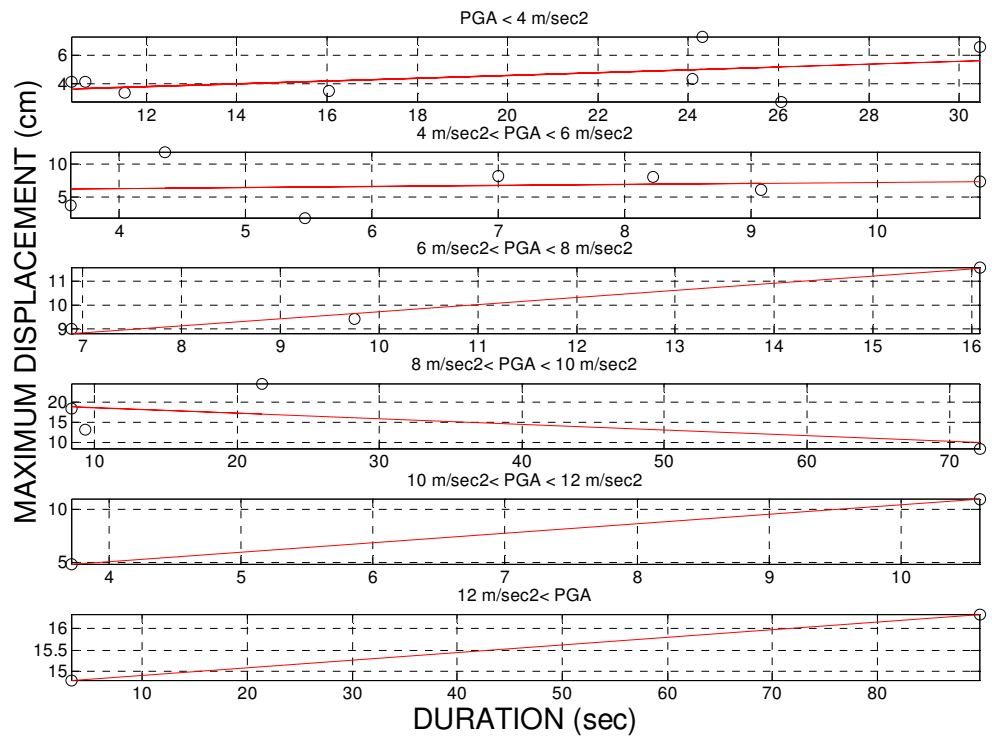


**Figure 4.7.** Max. Non-linear Displacement and SGMD relationship (frequency content of input motion is between 1.2-1.6 Hz)

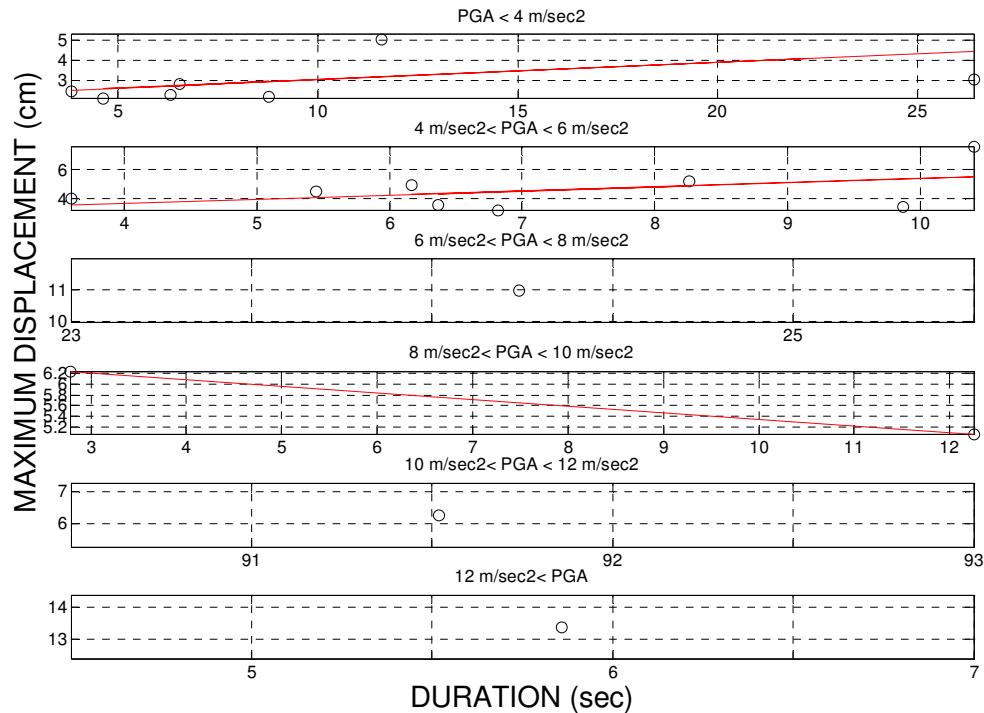


**Figure 4.8.** Max. Non-linear Displacement and SGMD relationship (frequency content of input motion is between 1.6-2.0 Hz)

## 5. CONCLUSION

In general, there is a positive correlation between SGMD and damage; however, in some PGA and frequency ranges, input motions with shorter durations may cause more damage than input motions with longer durations e.g. Parkfield (2004) with SGMD of 7 seconds vs. Japan-b (2011) with SGMD of 32 seconds in Figure 4.6.b; Chi-Chi (1999) with SGMD of 22 seconds vs. Tohoku (2011) with SGMD of 72 seconds in Figure 4.7.d. The main reason for this is that peak and predominant frequencies of the Japanese earthquakes are significantly different e.g. Japan-b has a peak frequency of 1.1 Hz and predominant frequency of 6.6 Hz; Tohoku has a peak frequency of 1.6 Hz and predominant frequency of 4.8 Hz. Determination of frequency content is important especially for broadband type input motions i.e. input motions where peak and predominant frequencies are significantly different; so that they are grouped into correct frequency range. Before making more definitive conclusions, SDOF systems with different initial natural frequencies; non-linear models considering strength degradation and P- $\Delta$  effects should be considered. These will be done in the near future.

## REFERENCES

- Chai, Y.H. (2005). Incorporating low-cycle fatigue model into duration-dependent inelastic design spectra. *Earthquake Engineering and Structural Dynamics*, **34**:1,83-06.
- Dutta, A. and Mander, J.B. (2001). Energy based methodology for ductile design of concrete columns. *Journal of Structural Engineering*, **127**:12,1374-1381.
- Erberik, M.A. and Sucuoglu, H. (2002). Seismic energy dissipation in deteriorating systems through low-cycle fatigue. *Earthquake Engineering and Structural Dynamics*, **33**:1,49-67.
- Fajfar, P., Vidic, T. and Fischinger, J. (1989). Seismic demand in medium and long period structures. *Earthquake Engineering and Structural Dynamics*, **18**:8,1133-1144.
- Hancock, J. and Bommer, J.J. (2006). A State-of-Knowledge Review of the Influence of Strong-Motion Duration on Structural Damage. *Earthquake Spectra*, **22**:3,827-845.
- Housner, G. W., 1956. Limit design of structures to resist earthquakes, *World Conference on Earthquake*

*Engineering, Berkeley, U.S.*

- Iervolino, I., Manfredi, G., and Cosenza, E. (2006). Ground motion duration effects on nonlinear seismic response, *Earthquake Engineering and Structural Dynamics*, **35**:1,21-38.
- Krawinkler, H. (1987). Performance assessment of steel components. *Earthquake Spectra*, 3:1,27-41.
- Park, Y., Ang, A.H. and Wen, Y.K. (1985). Seismic damage analysis of reinforced concrete buildings. *Journal of Structural Engineering*, **111**:4,740-757.
- Safak, E. (1998). 3D response spectra: A method to include duration in response spectra, *11<sup>th</sup> European Conference on Earthquake Engineering, Paris, France*.
- Uang, C.M. and Bertero, V.V. (1990). Evaluation of seismic energy in structures. *Earthquake Engineering and Structural Dynamics*, **19**:1,77-90.